*Microscopy and Microanalysis* (2019), **25**, 950–960
doi:10.1017/S1431927619000679

Microscopy AND Microanalysis

**Original Article**

# Annexin A2 Enhances the Progression of Colorectal Cancer and Hepatocarcinoma via Cytoskeleton Structural Rearrangements

Huimin He[1], Li Xiao[1], Sinan Cheng[1], Qian Yang[1], Jinmei Li[1], Yifan Hou[1], Fengying Song[1], Xiaorong Su[1], Huijuan Jin[1], Zheng Liu[1], Jing Dong[1], Ruiye Zuo[1], Xigui Song[1], Yanyan Wang[1], Kun Zhang[1], Wei Duan[2] and Yingchun Hou[1]*

[1]Department of Cell Biology, College of Life Sciences, Shaanxi Normal University, 620 West Chang-An Ave, Xi'an, Shaanxi 710119, China and [2]School of Medicine, Deakin University, Waurn Ponds, VIC 3216, Australia

**Abstract**

Annexin A2 (ANXA2) is reported to be associated with cancer development. To investigate the roles ANXA2 plays during the development of cancer, the RNAi method was used to inhibit the ANXA2 expression in caco2 (human colorectal cancer cell line) and SMMC7721 (human hepatocarcinoma cell line) cells. The results showed that when the expression of ANXA2 was efficiently inhibited, the growth and motility of both cell lines were significantly decreased, and the development of the motility relevant microstructures, such as pseudopodia, filopodia, and the polymerization of microfilaments and microtubules were obviously inhibited. The cancer cell apoptosis was enhanced without obvious significance. The possible regulating pathway in the process was also predicted and discussed. Our results suggested that ANXA2 plays important roles in maintaining the malignancy of colorectal and hepatic cancer by enhancing the cell proliferation, motility, and development of the motility associated microstructures of cancer cells based on a possible complicated signal pathway.

**Key words:** Annexin A2 (ANXA2), cytoskeleton rearrangements, malignancy, motility, proliferation

(Received 8 January 2019; revised 12 April 2019; accepted 6 May 2019)

## Introduction

Annexins can bind to negatively charged phospholipids in a $Ca^{2+}$-dependent manner. Annexin A2 (ANXA2), an important member of the annexin family, has a conserved C-terminal core domain which is the $Ca^{2+}$-binding molecule. The N-terminal domain of ANXA2 molecule mediates the regulatory interactions with protein ligands and regulates the ANXA2-membrane association implicated with F-actin assembly and cell motility mediated by the actin cytoskeleton (Ling et al., 2004; Bydoun & Waisman, 2014; Lauritzen et al., 2015). ANXA2 exists as a monomer or a heterotetramer containing a S100A10 dimer (Bydoun & Waisman, 2014). Various physiological functions have been assigned to the expression and distribution of ANXA2 in cells, such as mitogenic signal transduction (Benaud et al., 2015), DNA synthesis and cell proliferation (Chiang et al., 1993), and membrane fusion during exocytosis and endocytosis (Fan et al., 2011; Wang et al., 2016). The over expression of ANXA2 was detected in the tumors of brain, liver, pancreas, cervical, lung, and colon (Vishwanatha et al., 1992; Clifton et al., 2006; Zhai et al., 2011; Zheng & Jaffee, 2012; Kantara et al., 2015; Ağababaoğlu et al., 2017).

Cell motility is a key phenotype to evaluate the ability of tumor cell metastasis and ANXA2 has been implied to regulate the behavior of cytoskeleton protein. In motile cells, ANXA2 is concentrated in dynamic actin-rich protrusions and the depletion of ANXA by siRNA leads to the accumulation of stress fibers and loss of protrusive and retractile activity. ANXA2 participates in actin barbed-end capping and can reduce the rate of G-actin polymerization. ANXA2 may directly interact with monomeric and polymerized actin and play an essential regulatory role in maintaining the plasticity of the dynamic membrane-associated actin cytoskeleton (Hayes et al., 2006). Besides, a series of evidence shows that protein kinase A (PKA) is involved in the process of actin cytoskeleton rearrangement. Activated PKA may phosphorylate ANXA2, and then cause the dissociation of ANXA2 from F-actin and loss of ANXA2's F-actin bundling activity and therefore disassemble the cytoskeleton. A previous in vitro study indicated that phosphorylated AIIt (ANXA2-S100A10 heterotetramer) could neither bind to F-actin nor bundle F-actin at the physiological levels of $Ca^{2+}$ (Borthwick et al., 2008). However, as one of the candidates of actin-binding proteins, ANXA2 has been reported to bind and bundle F-actin. This seems contradictory to the previous experiments in which AIIt is thought to sever F-actin filaments. It is possible that AIIt binds to the cytoskeleton, while phosphorylation of AIIt leads to the dissociation of AIIt from the cytoskeleton and thus disruption of the cytoskeleton (Singh et al., 2004). ANXA2 may enhance the proliferation and motility of tumor cells (Clifton et al., 2006; Zheng & Jaffee, 2012; Kantara et al., 2015), but its expression is reduced or lost in dysplasia and head and neck squamous cell carcinoma and prostate cancer cells (Pena-Alonso et al., 2008; Liu et al., 2003; Christensen et al., 2018), while the re-expression of ANXA2 can

*Author for correspondence: Yingchun Hou, E-mail: ychhou@snnu.edu.cn

Cite this article: He H *et al* (2019) Annexin A2 Enhances the Progression of Colorectal Cancer and Hepatocarcinoma via Cytoskeleton Structural Rearrangements. *Microsc Microanal* **25**, 950–960. doi:10.1017/S1431927619000679

inhibit prostate cancer cell migration (Liu et al., 2003). ANXA2 also engages in the suppression of the motility of Moloney sarcoma virus-transformed Madin-Darby canine kidney cells (Balch & Dedman, 1997). ANXA2 may play roles in the apoptosis pathway. Under serum withdrawal or cisplatin treatment, PP2A/GSK-3 and Omi/HtrA2 cause ANXA2 cleavage and then cell cycle inhibition and apoptosis occurs (Wang et al., 2009). Cells (Anip973 and AGZY83-a lung cancer cells) transfected with Ad-p53 were observed with more apoptotic cells using both flow cytometry and terminal deoxynucleotidyl transferase mediated dUTP nick-end labeling assays. In all these cells, ANXA2 was down-regulated, especially in Anip973 cells (Huang et al., 2008). Down-regulation of ANXA2 expression using siRNA inhibited the proliferation of BE1 cell line with highly metastatic ability (Huang et al., 2008). However, the detailed regulations of ANXA2 to the behaviors of different kinds of tumor cells need to be further studied and confirmed. Our study was designed to investigate the roles of ANXA2 in regulating the cell behaviors in colorectal carcinoma cells (caco2) and hepatocarcinoma cells (SMMC7721) using the RNAi method, and analyze the effects of ANXA2 expression on the proliferation, motility and apoptosis of both cell lines, as well as on the development of the motility relevant microstructures, such as pseudopodia, filopodia, and the polymerization of microfilaments and microtubules. The possible regulating pathway in the process was also predicted and discussed.

## Materials and Methods

### Cell Culture

The caco2 cell line was purchased from ATCC (Rockville, MD, USA), and the SMMC7721 cell line was from our lab's stock. Both cell lines were cultured in RPMI1640 medium supplemented with 10% fetal bovine serum (Invitrogen, CA, USA) at 37°C in a humidified incubator containing 5% $CO_2$. Cells were passaged three times at least and five times at most before transfection.

### siRNA Designation and Transfection

The siRNA (5′-TAGTATAGGCTTTGACAGACCC-3′, marked as siANXA2) targeting ANXA2 open reading frame sequence was designed and cloned into pU6H1-GFP plasmid by Biomics Biotechnologies Co. Ltd (Nantong, China). A scrambled siRNA (5′-GCATCTAAGGTATCGTTGTGGCTC-3′, marked as siRNA-scr) was cloned as a control. In total, $2 \times 10^5$ cells per well were seeded in six-well plates for 24 h before transfection. Lipofectamine™ 2000 (Invitrogen, NY, USA) was used to transfect cells following the manufacturer's protocol. The cultured cells were grouped as the siRNA group (transfected with siANXA2), siRNAscr group (transfected with $siRNA_{SCR}$), and WT group (no transfection). The experiments were repeated three times independently and the transfection efficiency was evaluated by the number of transfected cells with green fluorescent protein (GFP) expression in three random representative fields.

### Semi-Quantitative RT-PCR

Semi-quantitative reverse transcription-PCR (RT-PCR) was used for the detection of ANXA2 mRNA level and evaluation of the inhibition efficiency of ANXA2 expression. Cell samples were harvested at 72 h post transfection. The Biozol Kit (BIOER, Hangzhou, China) was used to isolate total RNA following the manufacturer's protocol. RNA samples were quantified by using a bio-photometer manufactured by Eppendorf Company (Hamburg, Germany). The first-strand cDNA was synthesized using 1 μg of total mRNA, 1 μg Oligo dT, 1 mM dNTPs, and 5 U avian reverse transcriptase (Ding Guo Biotech, Beijing, China) in the final volume of 20 μL at 42°C for 1 h. In total, 1.5 μL of cDNA was used as the template for PCR. The primers for the semi-quantitative RT-PCR study of ANXA2 was as follows: top: 5′-GCGTCTAATCCGACAGCA-3′, and bottom: 5′-GCCGACT-TCCTTCACCAT-3′. GAPDH was used as an endogenous control. The PCR was programed to 23 cycles with 48°C as annealing temperature. The densitometric analysis of PCR products on 1.5% agarose gels was implemented using Bandscan 4.30 software. The experiments were repeated three times independently.

### Western Blotting

The methods of cell culture and transfection are the same as above. The cell lysates were prepared from each dish at 72 h post transfection, and the total protein in each sample was quantified using a BCA protein assay kit (Applygen, Beijing, China). In total, 40 μg protein for each sample was subjected to a 10% sodium dodecyl sulfate-polyacrylamide gel and transferred to nitrocellulose membrane (PALL, CA, USA). The transferred membrane was incubated with an rabbit-anti human ANXA2 antibody (1:500, Santa Cruz Biotechnology, Inc., CA, USA) and a horseradish peroxidase (HRP) labeled goat-anti rabbit antibody (1:3,000, Beijing Biosynthesis Biotech, Beijing, China). GAPDH (1:1,600, Sangon Biotechnology, China) was used as an endogenous control to standardize results in western blot assay. The membrane was developed using an ECL Kit (Pierce, Shanghai, China) following the manufacture's instruction. The densitometric analysis of the protein bands was implemented using Bandscan 4.30 software. The experiments were repeated three times independently.

### Immunohistochemical Staining

The cell culture, group designation, and transfection were the same as above, but the cells were seeded on a sterilized coverglass in each well of six-well plates. The cells were rinsed with phosphate-buffered saline (PBS) three times at 72 h post transfection, fixed in 4% buffered paraformaldehyde for 15 min at room temperature, and treated with 0.3% Triton X-100 for 10 min and 3% $H_2O_2$ for 15 min to block the endogenous peroxidase activity. Afterward, the normal goat serum (1:10, Ding Guo Biotech, Beijing, China) was used to block the non-specific binding of immunoglobulin for 30 min. Then the cells were incubated with a rabbit-anti human ANXA2 antibody (1:200) at 37°C for 3 h and a goat anti-rabbit antibody (1:2,000, Ding Guo Biotech, Beijing, China) at room temperature for 2 h, and then treated with streptavidin/HRP (5 μg/mL, Ding Guo Biotech, Beijing, China) at room temperature for 30 min. Finally, the cells anchored to coverglasses were displayed by treating them with diamino-benzidine (1 × working solution, Ding Guo Biotech, Beijing, China) for 5–10 min, washed in distilled water briefly, dehydrated in gradient alcohol solutions, cleared with xylene, and observed under a microscope.

### Wound Healing Assay

The group designation and transfection were the same as above. The transfected cells were cultured to confluence or near confluence (>90%) in six-well plates. On the day of the assay, confluent

https://doi.org/10.1017/S1431927619000679 Published online by Cambridge University Press

monolayer cells were wounded using a 1 mL pipette tip linked to a vacuum pump and then washed three times with PBS to clear any cell debris and suspended cells. Then image of each circle-shaped wound area was captured at 24, 48, 72, and 96 h at the same wound position. The remained wound area at each time point was compared with its initial wound area in 0 h using software Gene tools (Syngene) and ImageJ (National Institutes of Health). The cell migration rate was calculated based on the following formula: Migration Rate = $(1 - A_t/A_0) \times 100\%$; $A_0$: the pixel number for the initial wound area; $A_t$: the pixel number for the remained wound area at a time point post transfection.

### Transwell Chamber Assay

Transwell chamber assay was used for the quantitative measurement of cell migration. Briefly, 8,000 cells at 48 h post-transfection resuspended in 200 $\mu$L serum-free medium were seeded on the top chamber of a 12-well Transwell with polycarbonate filters with a pore size of 8 $\mu$m (Corning Costar Incorporated, New York, USA), and cells were allowed to migrate toward complete growth media present in the lower chamber overnight. Non-migrated cells were removed from the upper surface of the membrane by gentle scrubbing with a cotton swab and cells that had migrated to the lower side of the membrane were fixed with methanol, stained with 0.1% crystal violet solution, then imaged and counted under a light microscope. Five representative fields were counted for each Transwell filter to quantify the migrated cells in each group.

### MTT Assay

Cell growth was detected by 3-[4,5-dimethylthiazol-2-yl]-2,5-diphenyltetrazolium bromide (MTT) assay. The logarithm growing cells were seeded in 96-well plates ($4 \times 10^3$ cells per well). The group designation was the same as mentioned above and each group included six wells. Each well was transfected using 0.5 $\mu$g plasmid DNA. In total, 20 $\mu$L MTT (5 mg/mL, Sigma, USA) was added into each well at 24, 48, 72, and 96 h post transfection, then the cells were incubated in an incubator at 37°C and 5% $CO_2$ for 5 h. dimethyl sulfoxide (150 $\mu$L per well) was added and the plate was gently shaken on a shaker for 10 min. The absorbance at 562 nm ($OD_{562}$) was read on a ELX800 ELISA reader (Bio-Tek, USA).

### Coomassie Brilliant Blue Staining

The group designation and transfection were the same as above, and cells were cultured in a six-well plate containing small coverglass slips in each well for 24 h before transfection. The cell covered slips were rinsed with PBS at 72 h post transfection, then fixed in 4% paraformaldehyde for 10 min, transparentized with 0.1% Triton X-100 for 5 min. After washing with PBS again, coomassie brilliant blue R-250 (Sigma) was added and incubated at room temperature for 45 min. The cells were imaged under an inverted optical microscope.

### Scanning Electron Microscope (SEM)

The methods of cell culture and transfection are the same as above. Cells were fixed in 2.5% glutaraldehyde (Sigma) at 4°C for 1 h, then dehydrated in gradient diluted ethanol. Finally, the cell-covered slips were imaged under a scanning electron microscope (Quanta200, Philips-FEI, Netherlands) following the manufacturer's protocol.

### Immunofluorescence Assay

The methods of cell culture and transfection are the same as above. At 72 h post transfection, the cells cultured on a small glass cover slip in serum-starved medium (for cell synchronization) were washed once with PBS and then fixed with 4% paraformaldehyde for 15 min followed by four PBS washes. The fixed cells were transparentized in 0.3% TritonX-100 for 5 min and blocked for 45 min in blocking buffer (1% BSA), the slips were incubated with a rabbit anti-human F-actin polyclonal antibody (1:200, Santa Cruz Biotechnology, Inc., CA, USA) or rabbit anti-human β-tubulin polyclonal antibody (1:200, Santa Cruz Biotechnology, Inc., CA, USA) for 1 h at 37°C, then the cells were visualized using an Alexa-fluor 488 or 594 conjugated antibody, and the nuclei were displayed using 4′,6-diamidino-2-phenylindole (DAPI) staining. Finally, the slips were imaged under a laser scanning confocal microscope (LSCM) (Leica TCS SP5, Germany).

### Apoptosis Assay

The methods for cell culture and transfection are the same as above. The cells were stained using the Hoechst33258 staining kit (KeyGEN Biotech, Beijing, China) following the manufacturer's instruction.

### Statistical Analysis

Data are expressed as mean ± SD and analyzed using Student's *t*-test by GraphPad Prism 5. $p < 0.05$ was considered significant. All experiments were independently repeated for at least three times.

## Results

### ANXA2 Expression was Significantly Inhibited in caco2 and SMMC7721 Cells

pU6H1-GFP vector was used to express sequences of siRNAs under a cytomegalovirus (CMV) promoter and GFP under a CMV promoter. GFP sequence was cloned downstream of siRNA and was co-expressed with siRNA (Fig. 1a). The optimal Lipofectamine™ 2000 transfection condition for cells was conducted according to the manufacturer's protocol. siRNA transfection efficiency was evaluated at 72 h post transfection to be over than 80% by counting the GFP-expressed cells (Fig. 1b). Semi-quantitative RT-PCR and western blotting were used here to detect ANXA2 expression levels in the transfected cells. The results from semi-quantitative RT-PCR showed that the ANXA2 mRNA levels in the siANXA2 groups for both cell lines were significantly inhibited at 72 h post transfection (Figs. 2a, 2b). The results from western blotting demonstrated that the ANXA2 protein levels in the siANXA2 groups for both cell lines were remarkably decreased at 72 h post transfection (Figs. 2c, 2d). The immunocytochemical staining results revealed that ANXA2 was expressed in both nucleus and cytoplasm in WT and $siRNA_{SCR}$ groups at 72 h post transfection, but in siANXA2 groups, ANXA2 expression was dramatically inhibited (Fig. 2e). Taken together, the results above confirmed that the ANXA2 expression can be significantly inhibited by the ANXA2 targeting siRNA transfection in both caco2 and SMMC7721 cell lines.

### ANXA2 Inhibition Reduced the Cell Motility Significantly

The effect of ANXA2 on the migrative ability on the both cell lines was investigated by the wound healing assay and transwell

https://doi.org/10.1017/S1431927619000679 Published online by Cambridge University Press

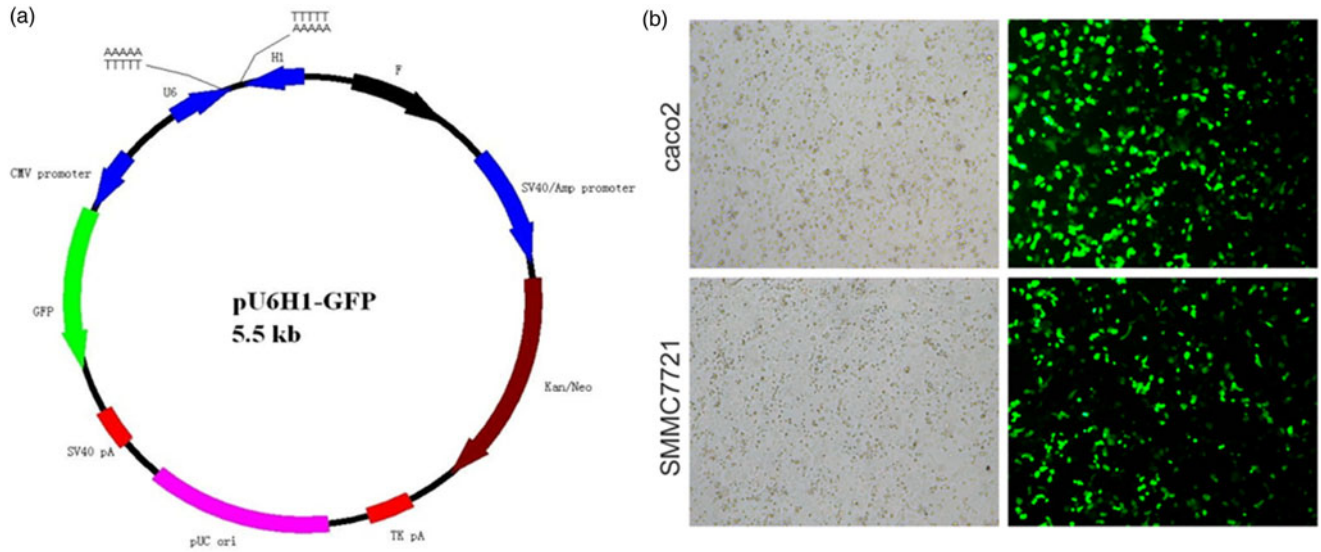


**Fig. 1.** Evaluation of siRNA transfection efficiency. **a:** Schematic map of plasmid pU6H1-GFP. **b**: Morphology of siRNA transfected caco2 and SMMC7721 cells. All light and fluorescent microscope images were taken following 72 h of transfection (×10).

chambers assay. To exclude the interference of the cell proliferation to the results, cycloheximide (Sigma, USA) was added into each of the wells at 24 h post transfection (working concentration: 10 $\mu$M). In both two cell lines the downregulation of ANXA2 expression significantly slowed the rate of wound closure, the migration rate of siANXA2-transfected cells was significantly decreased at 48, 72, and 96 h post transfection, especially comparing with the WT and siRNA$_{SCR}$ groups at 72 and 96 h post transfection (Figs. 3a, 3b). These results indicated that the cell motilities of both transfected cell lines were apparently inhibited because of the reduction of the ANXA2 expression level. The result of the transwell chambers assay at 48 h post transfection consistently showed lower migration ability in ANXA2 inhibited cells (Figs. 3c, 3d). Therefore, the inhibition of ANXA2 causes a decreased cell migration in both caco2 and SMMC7721 cell lines.

### ANXA2 Inhibition Decreased the Cell Growth Significantly

MTT assay was used to evaluate the cell proliferation. At 24 to 96 h post transfection, the absorbency of the siANXA2 group was reduced time-dependently, especially at 72 and 96 h post transfection. The downregulation of ANXA2 expression significantly inhibited the cell proliferation, the inhibitory rate of siANXA2 transfected cells was significantly increased in both two cell lines when comparing with the siRNA$_{SCR}$ group (Figs. 3e, 3f). These results indicated that the ANXA2 expression reduction in both caco2 and SMMC7721 cells causes the cell proliferation inhibition.

### ANXA2 Inhibition Suppressed the Development of Motility Relevant Microstructures

Recent studies raised the notion that motility relevant microstructures are closely associated with cell malignancy (Ribatti, 2017). We speculated that ANXA2 inhibition may cause the changes of motility relevant microstructures, especially the polymerization/depolymerization of microfilaments and microtubules in the pseudopodia and filopodia of cancer cells.

To investigate the effect of ANXA2 inhibition on cell microstructure regulation objectively, cell morphological changes were detected by coomassie brilliant blue staining and SEM microscopy. Images under an optic microscope show that ANXA2-inhibited cells exhibited a depleted development of pseudopodia/filopodia as determined by coomassie brilliant blue staining (Fig. 4a) and SEM microscopy (Fig. 4b), which might further disrupt the development of filopodia and pseudopodia in caco2 and SMMC7721 cells, suggesting a role of ANXA2 in the reorganization of the cytoskeleton. Cell contact inhibition, an important phenotype to evaluate the cancer cell malignancy displayed by SEM and coomassie brilliant blue staining, was re-induced in the ANXA2 inhibited group (Figs. 4a, 4b). Combining the results with the results from the transwell chamber assay and wound healing assay together, it is strongly indicated that ANXA2 enhances the cancer cell motility by remolding the motility relevant microstructures of cancer cells. The motility relevant microstructures were composed by actin and tubulin, and the level of polymerization/depolymerization of the both proteins is closely associated with cancer cell's motility (Pathak & Kumar, 2011; Gabel et al., 2019). Immunofluorescent staining images show depolymerized changes for microfilament (Figs. 5a, 5b) and microtubule (Figs. 6a, 6b) assembly in ANXA2 inhibited cells in both cell lines. These results suggest that the cytoskeleton undergoes reorganization in both caco2 and SMMC7721 cell lines after ANXA2 inhibition, suggesting an involvement of ANXA2 in the organization of cytoskeleton.

### ANXA2 Inhibition Affected the Cell Apoptosis Without Significance

Hoechst33258 staining is the method to evaluate cell apoptosis by identifying nuclear pyknosis. The results suggested that cell apoptosis remain unchanged after ANXA2 inhibition (Fig. 7). However, heteropythosis in ANXA2 inhibited cells was increased and similarly in both caco2 and SMMC7721 cell lines, which suggests that the cell apoptosis in the siANXA2 group was higher than that in other groups without significance at 72 h post transfection.

https://doi.org/10.1017/S1431927619000679 Published online by Cambridge University Press

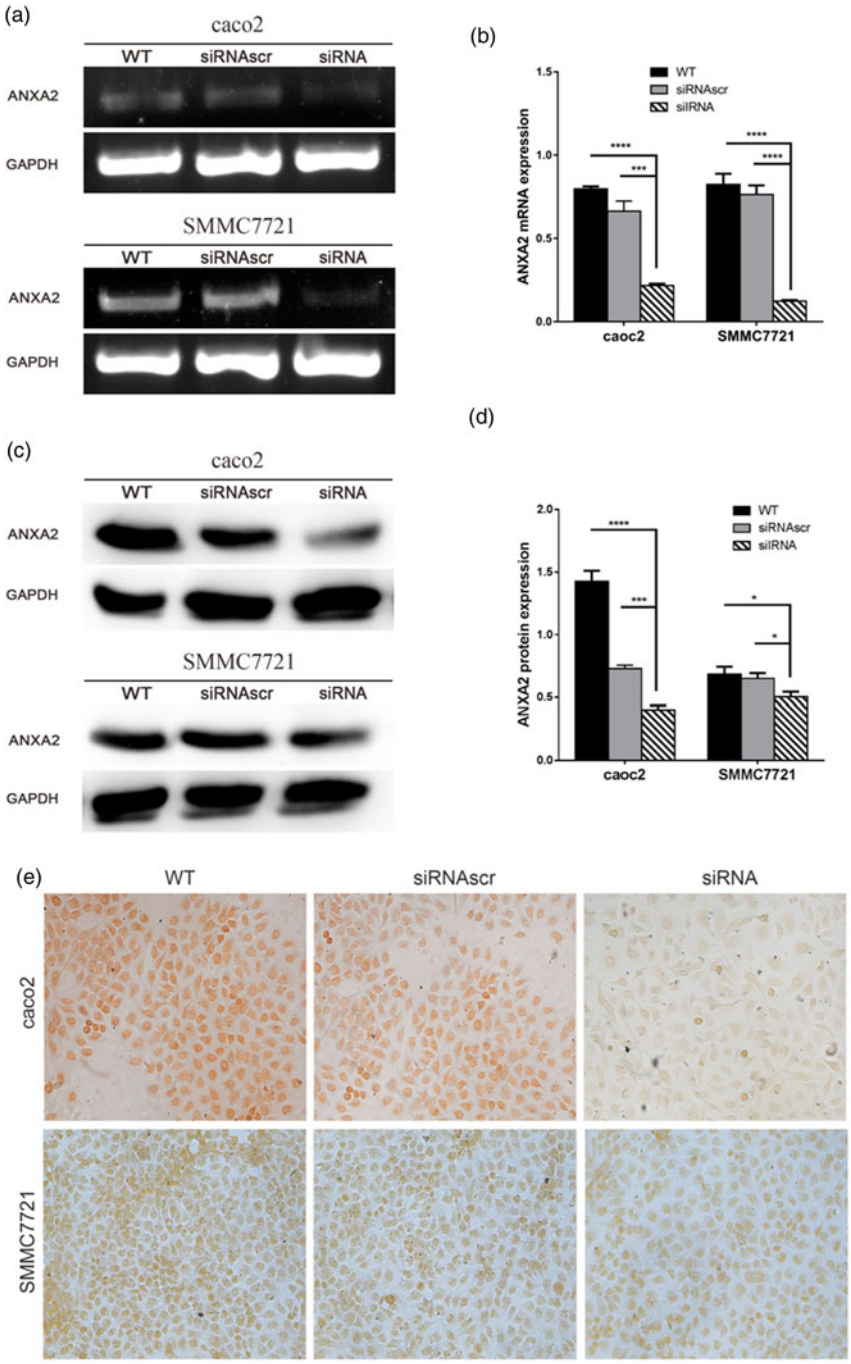


**Fig. 2.** Inhibition of ANXA2 generate attenuated mRNA and protein expression with significant in both caco2 and SMMC7721 cells. **a:** Changes of ANXA2 mRNA expression determined by semi-quantitative RT-PCR at 72 h post transfection. **b:** The quantification of ANXA2 expression at the mRNA level based on (**a**). **c**: Changes of ANXA2 protein expression determined by western blotting at 72 h post transfection. Total ANXA2 expression level was detected by an ANXA2 specific antibody that recognized the C-terminus of ANXA2. GAPDH is used for normalization. **d:** The quantification of ANXA2 expression at the protein level based on (**c**). **e:** ANXA2 (brown) expression measured by immunocytochemical staining at 72 h post transfection and the light microscope images were taken (×20). Double and triple asterisks denote $p$ value <0.01 and $p$ value <0.001, respectively.

## Discussion

ANXA2 is a calcium-dependent phospholipid binding protein (Siever & Erickson, 1997) and a primer recognition protein (PRP) (Vishwanatha et al., 1992) that has been abundantly presented at several malignances with various functional implications, many of which relevant to membrane trafficking and fusion (Gerke & Moss, 2002), fibrinolysis (Ling et al., 2004), inflammation (Defour et al., 2017), differentiation (Guzmán-Aránguez et al., 2005), metastatic ability (Kpetemey et al., 2015), and malignancy relevant microstructures (Jaiswal et al., 2014). ANXA2 activates DNA polymerase in lagging strand DNA synthesis (Chiang et al., 1993) and enhances DNA replication (Zheng & Jaffee, 2012). Interactions between tyrosine kinase receptors and cell-surface ANXA2 play an important role in the

https://doi.org/10.1017/S1431927619000679 Published online by Cambridge University Press

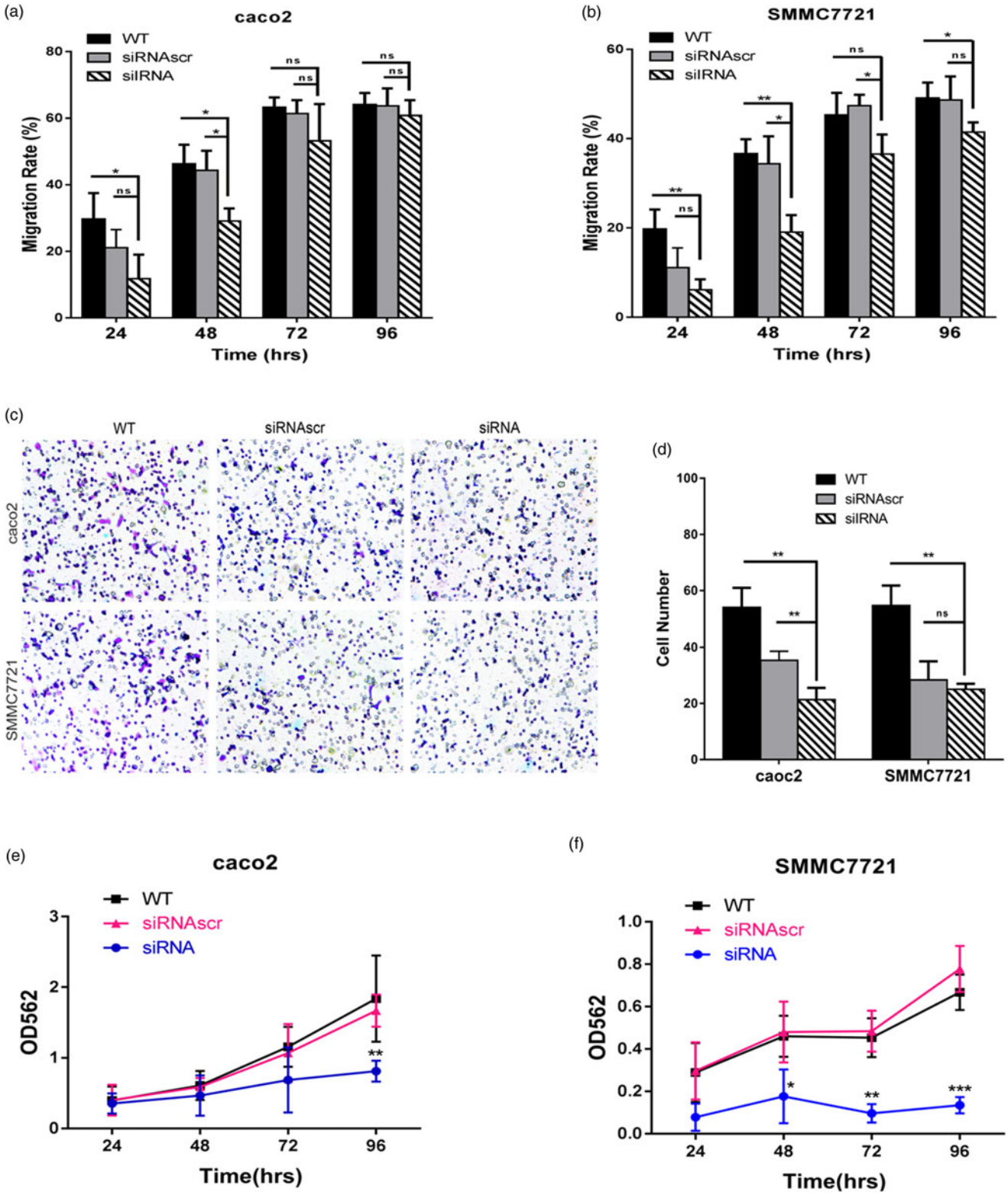


**Fig. 3.** Inhibition of ANXA2 depletes the cell motility and growth in caco2 and SMMC7721 cells. **a:** Measurement of cell motility by wound healing assay at different time points (24, 48, 72, and 96 h) in caco2 after cell transfection. **b:** Measurement of cell motility by wound healing assay at different time points (24, 48, 72, and 96 h) in SMMC7721 after cell transfection. **c:** Detection of cell migration by transwell chamber assay. Representative optical images were taken after crystal violet staining (×10). **d:** Quantification of migrated cells was evaluated by counting the number of cells in three random representative fields of the optical images. **e:** Evaluation of cell growth by MTT assay at different time points (24, 48, 72, and 96 h) in caco2 after cell transfection. **f:** Evaluation of cell growth by MTT assay at different time points (24, 48, 72, and 96 h) in SMMC7721 after cell transfection. Three biological replicates were performed in each experiment. The values were plotted as means ± SD ($n = 3$). Double and triple asterisks denote $p$ value <0.01 and $p$ value <0.001, respectively.

https://doi.org/10.1017/S1431927619000679 Published online by Cambridge University Press

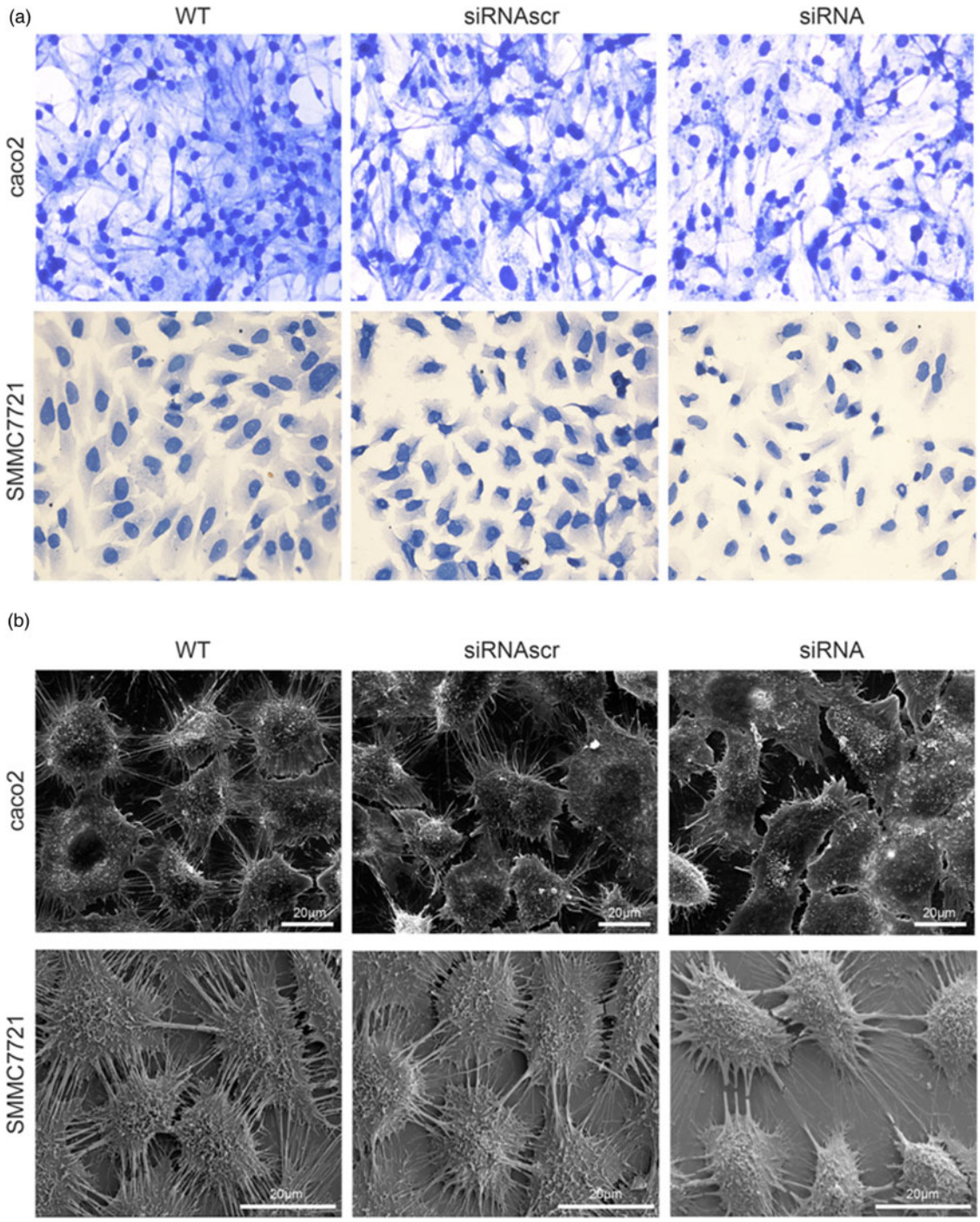


**Fig. 4.** Inhibition of ANXA2 regulates the cytoskeletal networks in caco2 and SMMC7721 cells. **a:** Representative light microscope images for coomassie brilliant blue staining at 72 h post transfection (×20). **b:** SEM observation of cytoskeletal networks at 72 h post transfection. Scale bars, 20 $\mu$m.

tumor microenvironment and act together to enhance tumor growth (Siever & Erickson, 1997). ANXA2 bridge disparate membranes and promote fusion in association with its binding partners (S100A10 and S100A11) (Chaudhary et al., 2014), which helps reseal the plasma membrane by facilitating polymerization of cortical F-actin and excision of the damaged part of the plasma membrane (Valapala & Vishwanatha, 2011; Demonbreun et al., 2016). Previous literature reported that ANXA2 is ubiquitously expressed in lung cancer (Jia et al., 2013), breast cancer (Jaiswal et al., 2014), pancreatic cancer (Maji et al., 2017), acute promyelocytic leukemia (Kwaan & Rego, 2010), colorectal carcinoma (Yamamoto et al., 2016), and hepatocarcinoma (El-Abd N et al., 2016), the up-regulation of ANXA2 is related to mitogenic signal transduction associated with several biological functions during the pathogenesis of cancers and the development of these malignancies (Christensen et al., 2018). Based on the description above, the up-regulated S100 and annexins in metastatic cancers and plasma membrane repair (PMR) (Jaiswal & Nylandsted, 2015) can be identified as the markers of metastatic cancers.

https://doi.org/10.1017/S1431927619000679 Published online by Cambridge University Press

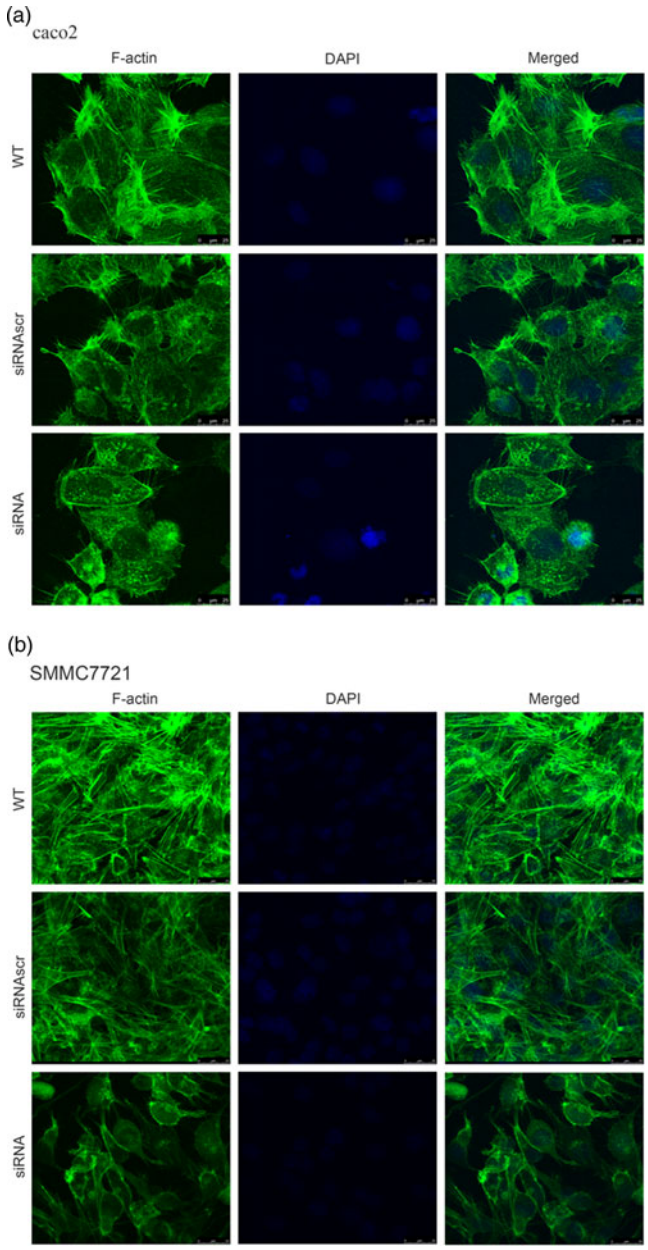


**Fig. 5.** Inhibition of ANXA2 induces F-actin rearrangements and presents a diffuse pattern of cytosolic localization in caco2 and SMMC7721 cells. **a:** Panels show F-actin (green) and DAPI (blue) immunofluorescent staining of caco2 at 72 h post transfection with siANXA2 or siRNAscr, or no transfection (WT). Scale bars, 25 $\mu$m. **b:** Panels show F-actin (green) and DAPI (blue) immunofluorescent staining of SMMC7721 at 72 h post transfection with siANXA2 or siRNAscr, or no transfection (WT). Scale bars, 25 $\mu$m.

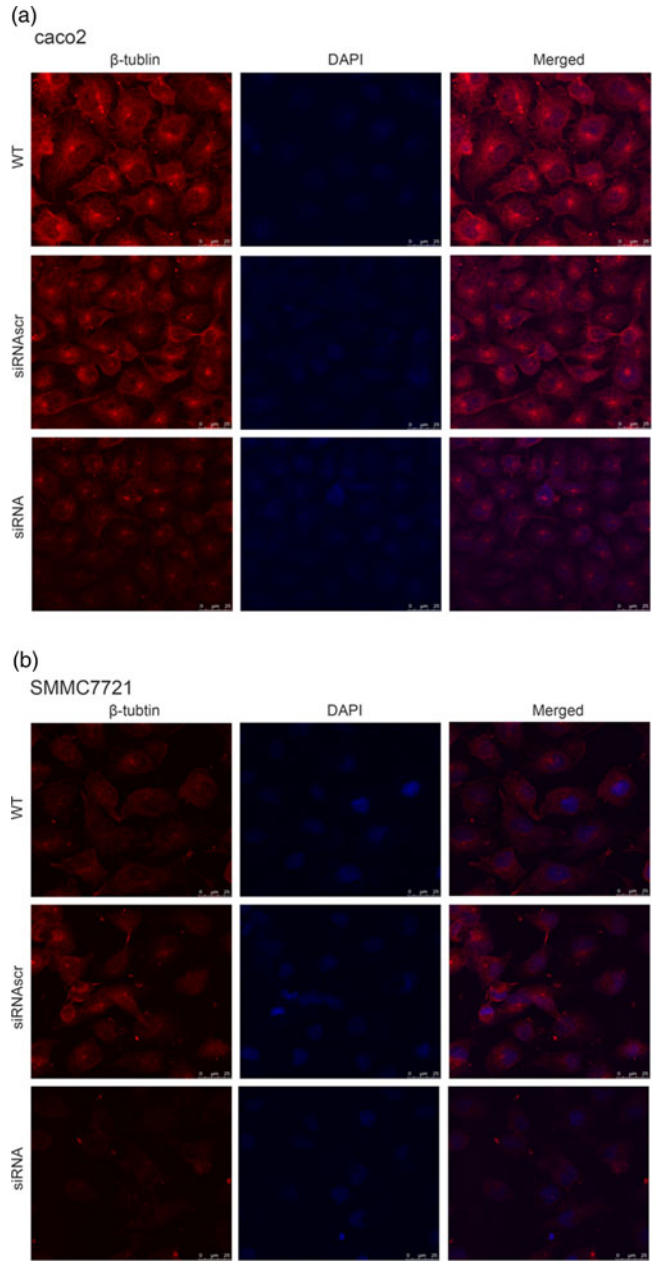


**Fig. 6.** Inhibition of ANXA2 modulates the formation and organization of β-tubulin in caco2 and SMMC7721 cells. **a:** Panels show β-tubulin (red) and DAPI (blue) immunofluorescent staining of caco2 at 72 h post transfection with siANXA2 or siRNAscr, or no transfection (WT). Scale bars, 100 $\mu$m. **b:** Panels showβ-tubulin (red) and DAPI (blue) immunofluorescent staining of SMMC7721 at 72 h post transfection with siANXA2 or siRNAscr, or no transfection (WT). Scale bars, 100 $\mu$m.

In an attempt to explore and confirm the roles ANXA2 plays in the development of colorectal carcinoma and hepatocarcinoma, we analyzed the cell proliferation, motility, and apoptosis of the caco2 and SMMC7721 cells when ANXA2 expression was inhibited via RNAi. Our results revealed that the inhibition of ANXA2 caused dramatic attenuation of cell proliferation (Figs. 3e, 3f) and motility (Figs. 3a–3d) in both cell lines, and indicated that enhanced expression of ANXA2 and its binding partner may be needed during the PRP (Vishwanatha et al., 1992) and PMR (Jaiswal & Nylandsted, 2015) for the high invasive ability in metastatic cancers. However, inhibition of ANXA2 failed to cause a significant cell apoptosis change (Fig. 7), and suggested that the inhibition just lead cells more susceptible to apoptotic stimuli only, such as serum withdrawal-induced cell cycle inhibition, cisplatin-induced apoptosis (Wang et al., 2009), or disrupted the construction of PRP (Vishwanatha et al., 1992), in spite of the fact that ANXA2 was reported to mildly enhance cell apoptosis and a weak heteropyknosis in ANXA2 inhibited cells was slightly presented in our results (Fig. 7). The findings above indicate that ANXA2 high expression is necessary to maintain the enhanced cell growth and motility for the high-metastatic potential of colorectal carcinoma and hepatocarcinoma.

https://doi.org/10.1017/S1431927619000679 Published online by Cambridge University Press

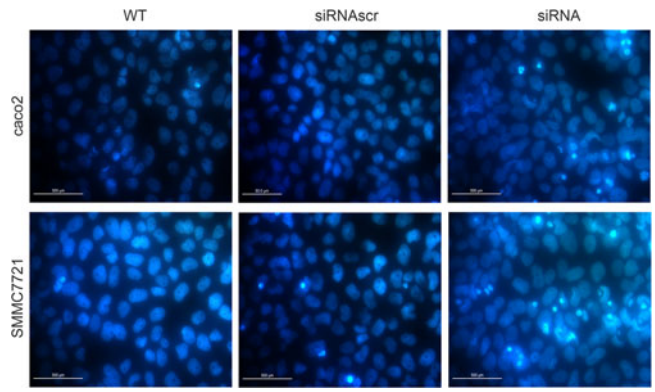


**Fig. 7.** Inhibition of ANXA2 had no significant influence on the apoptosis of caco2 and SMMC7721 cells. **a:** Detection of cell apoptosis by Hoechst33258 staining at 72 h post transfection in caco2 (×20). **b:** Detection of cell apoptosis by Hoechst33258 staining at 72 h post transfection in SMMC7721 (×20).

The change of microstructure and morphology is one of core major features of tumor malignancy, and it includes dramatic rearrangement of cytoskeletal networks, polymerized actin/actomyosin contractility, they both contribute to the enhanced motility of cancer cells (Sanz-Moreno & Marshall, 2010). However, these remain elusive in caco2 and SMMC7721 cells. Our results showed that the inhibition of ANXA2 caused the significant suppression of cell motility and recovery of cell contact inhibition in both cell lines (Fig. 4) based on the inhibition for the F-actin/tubulin expression and polymerization (Figs. 5, 6). These findings uncovered a critical role ANXA2 played in the coordination of cell motility relevant microstructures by enhancing the bind and bundle of F-actin (Filipenko & Waisman, 2001; Singh et al., 2004). Also its inhibition caused a weak F-actin polymerization and disassembly of cytoskeleton, that suggests the importance of ANXA2 to reorganize the cytoskeleton and enhance the motility in high-metastatic cancers. Tubulin is an important microtubule protein

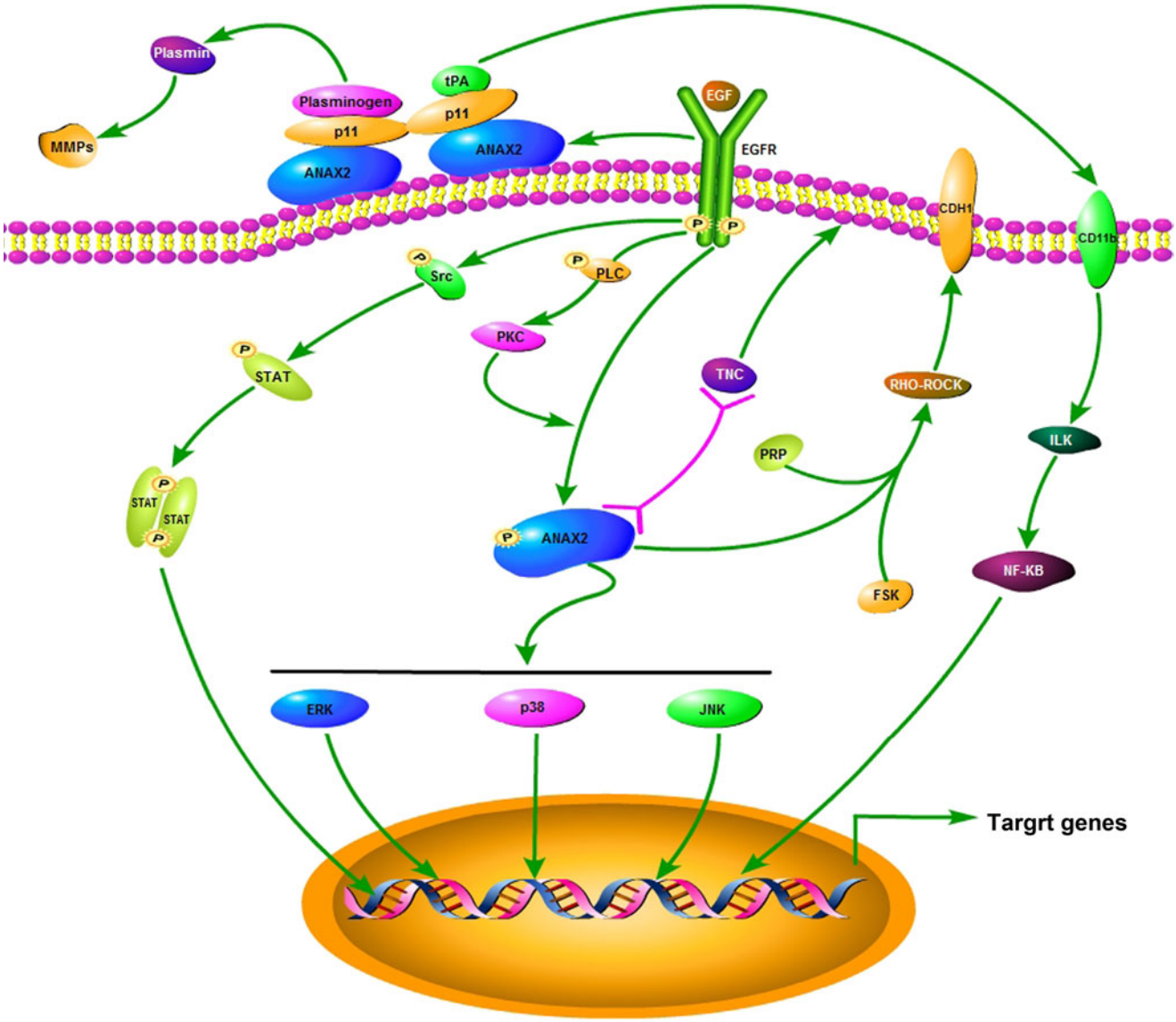


**Fig. 8.** A schematic diagram depicting a proposed signal pathway for ANXA2.

https://doi.org/10.1017/S1431927619000679 Published online by Cambridge University Press

to maintain the cytoskeleton-based cell motility (Pathak & Kumar, 2011; Gabel et al., 2019). Our results showed that ANXA2 inhibition suppressed the development of pseudopodia/filopodia and ceased the restoration of contact inhibition in both cell lines (Figs. 5, 6). These findings support that high ANXA2 expression enhances tubulin polymerization is also important to maintain the motility in high-metastatic cancers, and the lack of actin/tubulin polymerization is closely relevant to attenuation of extracellular matrix depended motility.

Based on the findings above, the regulation pathways for ANXA2 relevance to cancer cell malignancy may mediated by PKA (Borthwick et al., 2008), Src (Ma et al., 2018), Rho (Jolly et al., 2014), tenascin-C (Esposito et al., 2006), and procathepsin B (Mai et al., 2000) signals. ANXA2 can be activated by insulin receptor activation relevant to the actin accumulation and subsequent cell detachment (Rescher et al., 2008) associated with cancer metastasis. In this study, the morphological changes of cytoskeleton, especially the alternations of cell motility relevant microstructures induced by ANXA2 inhibition were investigated by LSCM and SEM microscopy. The results implied that the inhibition of ANXA2 expression could rearrange the cytoskeleton through the depletion of pseudopodia/filopodia and the disruption of F-actin and β-tubulin, and further affects the cancer malignancy via recovery of the cell contact inhibition. Combining our results and the references above, we proposed a possible signal regulation illustration in colorectal carcinoma or hepatocarcinoma in Figure 8.

## Conclusions

In summary, our findings support that elevated ANXA2 expression enhances the malignancy of caco2 and SMMC7721 cells by remodeling the cytoskeleton and motility associated microstructures, and maintaining cell proliferation at high level. The signals by which ANXA2 enhances the cancer malignancy may be merged to the pathways of mitogen-activated protein kinase, phosphatidylinositol 3-kinase, insulin, and nuclear factor-κB. Taken together, ANXA2 plays important role in enhancing the malignancy of colorectal carcinoma and hepatocarcinoma, and it has the potential to be used as a marker for the diagnosis or clinical evaluation to the both cancers, and also as a target for the gene target therapy of the both cancers. However, the detailed information about ANXA2 merged signal pathways during oncogenesis and cancer development should be subjected to further investigation.

**Acknowledgments.** We are grateful to Dr. Wei Duan for his writing suggestion and discussion; Dr. Xigui Song for his assistance with the statistical method during writing.

**Financial Support.** This work was supported by the Natural Scientific Foundation of Shaanxi Province (SJ08-ZT09); The China Grants for the Basic Researches in Central Universities (GK201704011); The China Grants for the Basic Researches in Central Universities (GK201704010).

**Conflict of Interest.** None.

## References

**Ağababaoğlu İ, Önen A, Demir AB, Aktaş S, Altun Z, Ersöz H, Şanl A, Özdemir N & Akkoçlu A** (2017). Chaperonin (HSP60) and annexin-2 are candidate biomarkers for non-small cell lung carcinoma. *Medicine (Baltimore)* **96**(6), e5903.

**Balch C & Dedman JR** (1997). Annexins II and V inhibit cell migration. *Exp Cell Res* **237**(2), 259–263.

**Benaud C, Le Dez G, Mironov S, Galli F, Reboutier D & Prigent C** (2015). Annexin A2 is required for the early steps of cytokinesis. *EMBO Rep* **16**(4), 481–489.

**Borthwick LA, Riemen C, Goddard C, Colledge WH, Mehta A, Gerke V & Muimo R** (2008). Defective formation of PKA/CnA-dependent annexin 2-S100A10/CFTR complex in DeltaF508 cystic fibrosis cells. *Cell Signal* **20**(6), 1073–1083.

**Bydoun M & Waisman DM** (2014). On the contribution of S100A10 and annexin A2 to plasminogen activation and oncogenesis: An enduring ambiguity. *Future Oncol* **10**(15), 2469–2479.

**Chaudhary P, Thamake SI, Shetty P & Vishwanatha JK** (2014). Inhibition of triple-negative and Herceptin-resistant breast cancer cell proliferation and migration by Annexin A2 antibodies. *Br J Cancer* **111**(12), 2328–2341.

**Chiang Y, Schneiderman MH & Vishwanatha JK** (1993). Annexin II expression is regulated during mammalian cell cycle. *Cancer Res* **53**(24), 6017–6021.

**Christensen MV, Høgdall CK, Jochumsen KM & Høgdall EVS** (2018). Annexin A2 and cancer: A systematic review. *Int J Oncol* **52**(1), 5–18.

**Clifton JG, Brown MK, Huang F, Li X, Reutter W, Hofmann W, Hixson DC & Josic D** (2006). Identification of members of the annexin family in the detergent-insoluble fraction of rat Morris hepatoma plasma membranes. *J Chromatogr A* **1123**(2), 205–211.

**Defour A, Medikayala S, Van der Meulen JH, Hogarth MW, Holdreith N, Malatras A, Duddy W, Boehler J, Nagaraju K & Jaiswal JK** (2017). Annexin A2 links poor myofiber repair with inflammation and adipogenic replacement of the injured muscle. *Hum Mol Genet* **26**(11), 1979–1991.

**Demonbreun AR, Quattrocelli M, Barefield DY, Allen MV, Swanson KE & McNally EM** (2016). An actin-dependent annexin complex mediates plasma membrane repair in muscle. *J Cell Biol* **213**(6), 705–718.

**El-Abd N, Fawzy A, Elbaz T & Hamdy S** (2016). Evaluation of annexin A2 and as potential biomarkers for hepatocellular carcinoma. *Tumour Biol* **37**(1), 211–216.

**Esposito I, Penzel R, Chaib-Harrireche M, Barcena U, Bergmann F, Riedl S, Kayed H, Giese N, Kleeff J, Friess H & Schirmacher P** (2006). Tenascin C and annexin II expression in the process of pancreatic carcinogenesis. *J Pathol* **208**(5), 673–685.

**Fan C, Fu Z, Su Q, Angelini DJ, Van Eyk J & Johns RA** (2011). S100a11 mediates hypoxia-induced mitogenic factor (HIMF)-induced smooth muscle cell migration, vesicular exocytosis, and nuclear activation. *Mol Cell Proteomics* **10**(3), M110.000901.

**Filipenko NR & Waisman DM** (2001). The C terminus of annexin II mediates binding to F-actin. *J Biol Chem* **276**(7), 5310–5315.

**Gabel M, Delavoie F, Royer C, Tahouly T, Gasman S, Bader MF, Vitale N & Chasserot-Golaz S** (2019). Phosphorylation cycling of Annexin A2 Tyr23 is critical for calcium-regulated exocytosis in neuroendocrine cells. *Biochim Biophys Acta Mol Cell Res* **1866**(7), 1207–1217.

**Gerke V & Moss SE** (2002). Annexins: From structure to function. *Physiol. Rev* **82**(2), 331–371.

**Guzmán-Aránguez A, Olmo N, Turnay J, Lecona E, Pérez-Ramos P, López de Silanes I & Lizarbe MA** (2005). Differentiation of human colon adenocarcinoma cells alters the expression and intracellular localization of annexins A1, A2, and A5. *J Cell Biochem* **94**(1), 178–193.

**Hayes MJ, Shao D, Bailly M & Moss SE** (2006). Regulation of actin dynamics by annexin 2. *EMBO J* **25**(9), 1816–1826.

**Huang Y, Jin Y, Yan CH, Yu Y, Bai J, Chen F, Zhao YZ & Fu SB** (2008). Involvement of Annexin A2 in p53 induced apoptosis in lung cancer. *Mol Cell Biochem* **309**(1–2), 117–123.

**Jaiswal JK, Lauritzen SP, Scheffer L, Sakaguchi M, Bunkenborg J, Simon SM, Kallunki T, Jäättelä M & Nylandsted J** (2014). S100a11 is required for efficient plasma membrane repair and survival of invasive cancer cells. *Nat Commun* **5**, 3795.

**Jaiswal JK & Nylandsted J** (2015). S100 and annexin proteins identify cell membrane damage as the Achilles heel of metastatic cancer cells. *Cell Cycle* **14**(4), 502–509.

**Jia JW, Li KL, Wu JX & Guo SL** (2013). Clinical significance of annexin II expression in human non-small cell lung cancer. *Tumour Biol* **34**(3), 1767–1771.

**Jolly C, Winfree S, Hansen B & Steele-Mortimer O** (2014). The Annexin A2/p11 complex is required for efficient invasion of *Salmonella* Typhimurium in epithelial cells. *Cell Microbiol* **16**(1), 64–77.

https://doi.org/10.1017/S1431927619000679 Published online by Cambridge University Press

**Kantara C, O'Connell MR, Luthra G, Gajjar A, Sarkar S, Ullrich RL & Singh P** (2015). Methods for detecting circulating cancer stem cells (CCSCs) as a novel approach for diagnosis of colon cancer relapse/metastasis. *Lab Invest* **95**(1), 100–112.

**Kpetemey M, Dasgupta S, Rajendiran S, Das S, Gibbs LD, Shetty P, Gryczynski Z & Vishwanatha JK** (2015). MIEN1, a novel interactor of Annexin A2, promotes tumor cell migration by enhancing AnxA2 cell surface expression. *Mol Cancer* **14**, 156.

**Kwaan HC & Rego EM** (2010). Role of microparticles in the hemostatic dysfunction in acute promyelocytic leukemia. *Semin Thromb Hemost* **36**(8), 917–924.

**Lauritzen SP, Boye TL & Nylandsted J** (2015). Annexins are instrumental for efficient plasma membrane repair in cancer cells. *Semin Cell Dev Biol* **45**, 32–38.

**Ling Q, Jacovina AT, Deora A, Febbraio M, Simantov R, Silverstein RL, Hempstead B, Mark WH & Hajjar KA** (2004). Annexin II regulates fibrin homeostasis and neoangiogenesis in vivo. *J Clin Invest* **113**(1), 38–48.

**Liu J-W, Shen J-J, Tanzillo-Swarts A, Bhatia B, Maldonado CM, Person MD, Lau SS & Tang DG** (2003). Annexin II expression is reduced or lost in prostate cancer cells and its re-expression inhibits prostate cancer cell migration. *Oncogene* **22**(10), 1475–1485.

**Ma S, Lu CC, Yang LY, Wang JJ, Wang BS, Cai HQ, Hao JJ, Xu X, Cai Y, Zhang Y & Wang MR** (2018). ANXA2 promotes esophageal cancer progression by activating MYC-HIF1A-VEGF axis. *J Exp Clin Cancer Res* **37**(1), 183.

**Mai J, Finley Jr RL, Waisman DM & Sloane BF** (2000). Human procathepsin B interacts with the annexin II tetramer on the surface of tumor cells. *J Biol Chem* **275**(17), 12806–12812.

**Maji S, Chaudhary P, Akopova I, Nguyen PM, Hare RJ, Gryczynski I & Vishwanatha JK** (2017). Exosomal Annexin II promotes angiogenesis and breast cancer metastasis. *Mol Cancer Res* **15**(1), 93–105.

**Pathak A & Kumar S** (2011). Biophysical regulation of tumor cell invasion: Moving beyond matrix stiffness. *Integr Biol (Camb)* **3**(4), 267–278.

**Pena-Alonso E, Rodrigo JP, Parra IC, Pedrero JM, Meana MV, Nieto CS, Fresno MF, Morgan RO & Fernandez MP** (2008). Annexin A2 localizes to the basal epithelial layer and is down-regulated in dysplasia and head and neck squamous cell carcinoma. *Cancer Lett* **263**(1), 89–98.

**Rescher U, Ludwig C, Konietzko V, Kharitonenkov A & Gerke V** (2008). Tyrosine phosphorylation of annexin A2 regulates Rho-mediated actin rearrangement and cell adhesion. *J Cell Sci* **121**(Pt 13), 2177–2185.

**Ribatti D** (2017). A revisited concept: Contact inhibition of growth. From cell biology to malignancy. *Exp Cell Res* **359**(1), 17–19.

**Sanz-Moreno V & Marshall CJ** (2010). The plasticity of cytoskeletal dynamics underlying neoplastic cell migration. *Curr Opin Cell Biol* **22**(5), 690–696.

**Siever DA & Erickson HP** (1997). Extracellular annexin II. *Int J Biochem Cell Biol* **29**(11), 1219–1223.

**Singh TK, Abonyo B, Narasaraju TA & Liu L** (2004). Reorganization of cytoskeleton during surfactant secretion in lung type II cells: A role of annexin II. *Cell Signal* **16**(1), 63–70.

**Valapala M & Vishwanatha JK** (2011). Lipid raft endocytosis and exosomal transport facilitate extracellular trafficking of annexin A2. *J Biol Chem* **286**(35), 30911–30925.

**Vishwanatha JK, Jindal HK & Davis RG** (1992). The role of primer recognition proteins in DNA replication: Association with nuclear matrix in HeLa cells. *J Cell Sci* **101**(Pt 1), 25–34.

**Wang CY, Lin YS, Su WC, Chen CL & Lin CF** (2009). Glycogen synthase kinase-3 and Omi/HtrA2 induce annexin A2 cleavage followed by cell cycle inhibition and apoptosis. *Mol Biol Cell* **20**(19), 4153–4161.

**Wang S, Sun H, M Tanowitz, X-H Liang & Stanley T** (2016). Crooke. Annexin A2 facilitates endocytic trafficking of antisense oligonucleotides. *Nucleic Acids Res* **44**(15), 7314–7330.

**Yamamoto T, Kudo M, Peng WX, Takata H, Takakura H, Teduka K, Fujii T, Mitamura K, Taga A, Uchida E & Naito Z** (2016). Identification of aldolase A as a potential diagnostic biomarker for colorectal cancer based on proteomic analysis using formalin-fixed paraffin-embedded tissue. *Tumour Biol* **37**(10), 13595–13606.

**Zhai H, Acharya S, Gravanis I, Mehmood S, Seidman RJ, Shroyer KR, Hajjar KA & Tsirka SE** (2011). Annexin A2 promotes glioma cell invasion and tumor progression. *J Neurosci* **31**(40), 14346–14360.

**Zheng L & Jaffee EM** (2012). Annexin A2 is a new antigenic target for pancreatic cancer immunotherapy. *Oncoimmunology* **1**(1), 112–114.

https://doi.org/10.1017/S1431927619000679 Published online by Cambridge University Press